

# Combining ERPs and EEG Spectral Features for Decoding Intended Movement Direction\*

Junhua Li, *Student Member, IEEE*, Yijun Wang\*, *Member, IEEE*, Liqing Zhang, and Tzyy-Ping Jung, *Senior Member, IEEE*

**Abstract**—The posterior parietal cortex (PPC) plays an important role in visuomotor transformations for movement planning and execution. To investigate how noninvasive electroencephalographic (EEG) signals correlate with intended movement directions in the PPC, this study recorded whole-head EEG during a delayed saccade-or-reach task and found direction-related changes in both event-related potentials (ERPs) and the EEG power in the theta and alpha bands in the PPC. Single-trial (left versus right) classification using ERP and EEG spectral features prior to motor execution obtained an average accuracy of 65.4% and 65.6% respectively on 10 subjects. By combining the two types of features, the classification accuracy increased to 69.7%. These results show that ERP and EEG spectral power modulations contribute complementary information to decoding intended movement directions in the PPC. The proposed paradigm might lead to a practical brain-computer interface (BCI) for decoding movement intention of individuals.

## I. INTRODUCTION

Neural decoding of movement intention has been widely studied in the area of brain-machine interface (BMI) based neuroprosthetics [1]. For example, neuronal activities recorded in the primary motor cortex (M1) of monkey and human subjects, where neuron-firing patterns encode direction information about limb movement, can be used to predict the outcomes of planned actions [2-4]. It is also well known that the posterior parietal cortex (PPC) plays an important role in movement planning, being involved in sensorimotor transformations from visual input to motor execution. Recently, in monkey studies, direction decoding of eye and hand movements has been realized using neuronal signals in the PPC [5]. However, in human studies, movement direction decoding using noninvasive methods has not been widely studied [6-8]. To the best of our knowledge, direction decoding based on scalp EEG recordings is ignored in current brain-computer interface (BCI) research.

In the PPC areas, two neural processes, which might contribute to predicting intended movement direction, are involved in movement planning. The first is the visuomotor transformation, which is crucial for transforming visual

signals into motor commands. Our previous study [8] reported that ERP components, which might reflect the early visuomotor transformations of movement directions, exhibited a contralateral decrease and ipsilateral increase in amplitudes during 180-350ms after the appearance of the visual direction cue. In the study, we applied a single-trial classification method to decode intended movement direction using only temporal ERP features from the PPC areas and achieved classification accuracy significantly higher than the chance level in four subjects [8]. The second neural process that involves in movement planning is visuospatial attention, which is important for directing spatial attention to the targets before motor execution. Previous studies showed that the direction of visuospatial attention could be predicted by measuring EEG alpha power over the two posterior hemispheres [9]. Therefore, attention-related EEG spectra preceding motor actions could be used to improve the accuracy of predicting movement directions.

This study investigates spatiotemporal EEG dynamics in the human PPC during directional movement planning. This study also examines whether EEG power changes can complement the temporal ERP waveforms for decoding movement direction. To this end, this study proposes a feature combination scheme for decoding intended movement direction based on single-trial EEG data.

## II. METHODS

### A. Stimuli and Procedure

This study used a delayed saccade-or-reach task, which allowed us to look for direction specific information in the EEG during the phase of movement planning. Subjects were seated comfortably in an armchair at a distance of 40cm from a 19-inch touch screen. A chin rest was used to help them maintain head position.

Subjects used their right hand to perform reach tasks. At the beginning of each trial, the subject's forearm rested on the table with the index finger holding down a key on a keypad placed 30cm in front of screen center. Fig. 1 shows the sequence of visual cues in each trial. At the beginning of each trial, a fixation cross ( $0.65^\circ \times 0.65^\circ$ ) was displayed in the center of the screen plus three red crosses ( $0.65^\circ \times 0.65^\circ$ ) indicating potential target positions. The left and right targets had a vertical distance of  $6^\circ$  and a horizontal distance of  $15^\circ$  from the central fixation cross; the central target was  $12^\circ$  upwards. After 500ms, an effector cue ( $0.5^\circ \times 0.5^\circ$ , rectangle, ellipse, and a mixture of them indicating hand, eye, and two-effector movements respectively) appeared at screen center for 1000ms. Next, a central direction cue ( $0.65^\circ \times 0.65^\circ$ ,  $\leftarrow$ ,  $\uparrow$ ,  $\rightarrow$  for left, upward, and right respectively) was presented for

\*Research is supported in part by a gift fund from Abraxis Bioscience Inc., National Natural Science Foundation of China (Grant No. 90920014, 91120305), US Army Research Laboratory, Army Research Office, DARPA and Office of Naval Research.

J. Li and L. Zhang are with Shanghai Jiao Tong University, Shanghai, 200240 China (e-mail: juhalee@sjtu.edu.cn, zhang-lq@cs.sjtu.edu.cn)

\*Y. Wang and T.-P. Jung are with University of California San Diego, San Diego, CA 92093 USA (phone: 858-822-7550; fax: 858-822-7556; e-mail: yijun@scn.ucsd.edu, jung@scn.ucsd.edu).

700ms. Subjects were asked to maintain fixation on the central cue until they started their response, to perform the indicated response as quickly as possible after the direction cue disappeared, and finally to return to their initial (key-down) position. Total trial duration amounted to 3500~4000ms.

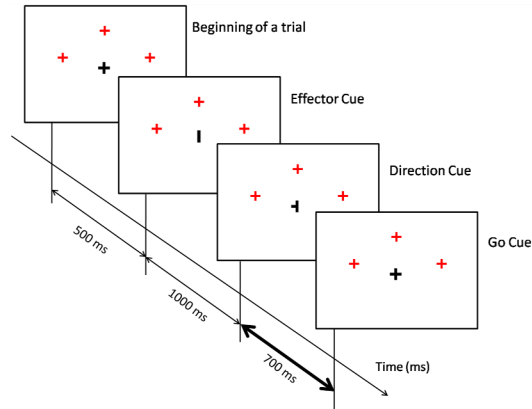


Figure 1. Time sequences of cue presentation in a trial. In each trial, three central cues (first, effector cue, next, direction cue, and finally, go cue) were presented. The 700 ms delay period between the “Direction cue” and “Go cue” was considered the phase of directional movement planning.

### B. Data Acquisition

Ten healthy, right-handed participants (7 males and 3 females) with normal or corrected-to-normal vision performed this experiment. All participants were asked to read and sign an informed consent form approved by the UCSD Human Research Protections Program before participating in the study.

EEG data were recorded using Ag/AgCl electrodes from 128 scalp positions distributed over the entire scalp using a BioSemi ActiveTwo EEG system (Biosemi, Inc.). Eye movements were monitored by additional bipolar horizontal and vertical EOG electrodes. Electrode locations were measured with a 3-D digitizer system (Polhemus, Inc.). Three cue presentation events and two manual response events (“button release” and “screen touch”) were recorded on an event channel synchronized to the EEG data. All signals were amplified and digitized at a sample rate of 256 Hz. The experiment consisted of four blocks (with breaks in between) each including five runs of 45 trials. Within each block, there was a 20-second rest between runs. A total of 900 trials were equally distributed among the nine tasks, which were presented to the subjects in a pseudorandom sequence.

### C. Data Preprocessing

This study focuses on the estimations of planned direction of movement. For simplicity, this study focuses on “left” and “right” conditions for “hand” tasks. The same analysis could be applied to data under “eye” and “both” conditions. Epochs from the response delay period, 0 to 700ms following the onsets of direction cues, were extracted from the continuous data, and labeled by movement directions. The period [-100ms 0] was used as the baseline for each trial. Electrodes with poor skin contact were identified by their abnormal activity patterns and removed from the data.

We used independent component analysis (ICA) as an unsupervised spatial filtering technique to remove artifacts

arising from eye and muscle movements [10]. All trials were band-pass filtered (1-30 Hz), concatenated, and then decomposed using the ICA function of the EEGLAB toolbox [11]. To retain the low-frequency EEG activities, ICA weights of the decomposition were applied to original unfiltered data before artifact removal.

### D. Feature Extraction and Classification

The location of source activities related to the intended movement direction can be estimated by source localization of the two lateralized PPC components extracted by ICA [8]. Fourteen channels (seven channels on each hemisphere) around the estimated sources were used for feature extraction. We adopted ERP features, EEG spectral features, and the combination of those two types of features to classify the intended movement directions (i.e., reach left vs. reach right) respectively. A support vector machine (SVM) [12] classifier was employed for classification.

#### (1) ERP features

ERP signals from the PPC areas showed a contralateral decrease and ipsilateral increase during movement planning. Therefore, temporal ERP amplitudes can be directly used as features for distinguishing the left and right movement directions. To improve the signal-to-noise ratio (SNR) of ERPs and reduce the feature dimension at the same time, we employed the canonical correlation analysis (CCA) [13] algorithm to design spatial filters. Here, CCA sought channel weights, which aimed to maximize the correlation between the projection of all seven channels and that of the three channels in the central region of the PPC area, for the left and right hemispheres respectively. The spatial filtering procedure can be described as

$$Z = W * X \quad (1)$$

where  $X$  is the multi-channel EEG signal of a trial and  $W$  is the CCA-based spatial filter. We obtained two projected vectors  $Z_L$  and  $Z_R$ , which corresponded to electrodes on the left and right hemispheres, after spatial filtering. To further reduce feature dimension,  $Z_L$  and  $Z_R$  were downsampled by calculating the mean of five continuous data points without overlapping. Finally,  $Z_L$  and  $Z_R$  were concatenated together to form a feature vector as

$$V_{\text{ERP}} = [Z_L \ Z_R]^T \quad (2)$$

#### (2) EEG spectral power features

We adopted short-time Fourier transform [14] to convert EEG time series into a time-frequency representation of the data. For each channel, the data were transformed to spectral domain using a 250-ms time window, which moved through each trial in 15.625-ms (i.e., four data points) steps. Then, a time-frequency distribution matrix can be obtained as

$$Y(f, t) = \begin{bmatrix} y_{f_1 t_1} & y_{f_1 t_2} & \cdots & y_{f_1 t_n} \\ y_{f_2 t_1} & y_{f_2 t_2} & \cdots & y_{f_2 t_n} \\ \vdots & \vdots & \ddots & \vdots \\ y_{f_m t_1} & y_{f_m t_2} & \cdots & y_{f_m t_n} \end{bmatrix} \quad (3)$$

where frequency increases across the rows from  $f_1$  to  $f_m$ , and time increases across the columns from  $t_1$  to  $t_n$ , so that each element  $y_{f_i t_j}$  in the matrix is the value of EEG power at frequency  $f_i$  and time  $t_j$ . Considering the individual difference of time-frequency distributions of spectral features under different conditions, we chose subject specific parameters to obtain a submatrix

$$Y_{\text{Sub}}(f, t) = \begin{bmatrix} y_{f_{s1}t_{s1}} & \cdots & y_{f_{s1}t_{s_q}} \\ \vdots & \ddots & \vdots \\ y_{f_{s_p}t_{s1}} & \cdots & y_{f_{s_p}t_{s_q}} \end{bmatrix} \quad (4)$$

where the frequency ranges from  $f_{s1}$  to  $f_{s_p}$ , and the time period from  $t_{s1}$  to  $t_{s_q}$ . To reduce the feature dimension, all frequency elements in each column were summed up to form a vector

$$Y = [y_{t_{s1}} \ y_{t_{s2}} \ \cdots \ y_{t_{s_q}}] \quad (5)$$

where

$$y_{t_{s_i}} = y_{f_{s1}t_{s_i}} + y_{f_{s2}t_{s_i}} + \cdots + y_{f_{s_k}t_{s_i}} \quad (6)$$

The processing procedure above was performed for all the channels. Then, in each hemisphere, the feature vectors of all channels were summed up to obtain a feature vector as follows:

$$Y_{L/R} = [\bar{y}_{t_{s1}} \ \bar{y}_{t_{s2}} \ \cdots \ \bar{y}_{t_{s_q}}] \quad (7)$$

where

$$\bar{y}_{t_{s_i}} = y_{D_1 t_{s_i}} + y_{D_2 t_{s_i}} + \cdots + y_{D_k t_{s_i}} \quad (8)$$

$D$  indicates the channel index ( $D \in \{E_L, E_R\}$ ,  $E_L$  and  $E_R$  represent the selected channels on the left and right hemispheres respectively) and  $k$  is the number of channels on each hemisphere. Finally, the two feature vectors corresponding to electrodes on the left and right hemispheres were concatenated together to form a feature vector

$$V_{\text{Power}} = [Y_L \ Y_R]^T \quad (9)$$

### (3) Feature combination

We assumed that feature combination might improve overall classification accuracy because the temporal ERP features can be complementary to the spectral power features. Hence, we fused the ERP features and the power features by simply concatenating them as

$$V_{\text{Combination}} = [V_{\text{ERP}} \ V_{\text{Power}}]^T \quad (10)$$

### (4) Classification

The resultant feature vector was fed into an SVM classifier using a radial basis function kernel. The SVM algorithm was performed in the MATLAB® Bioinformatics Toolbox. 10-fold cross validation was conducted to estimate classification performance.

## III. RESULTS

### A. ERP Modulation

To extract the direction-specific activity of the ERPs, we compared the spatiotemporal patterns of EEG difference waves between the left and right movement directions. As shown in Fig. 2, a hemispheric asymmetry over the parietal cortex during the delay period in which motor planning can be presumed to have continued until the cued movement onset. Activities in the PPC areas showed a significant contralateral negativity and ipsilateral positivity with respect to the intended movement direction. Across all subjects, the difference waves between the reaching left and reaching right conditions showed two peaks located at 200ms and 320ms following the direction cue. At a later stage around 440ms, the difference waves also showed some activities at the medial frontal and parietal areas.

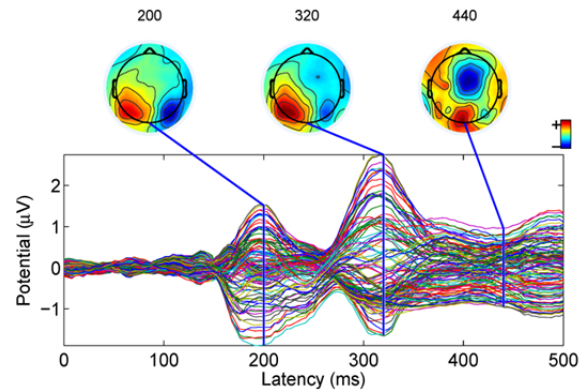


Figure 2. Scalp maps and temporal waveforms of the difference waves between the left and right direction conditions. The difference waves showed two peaks at 200ms and 320ms after the direction cue, indicating a contralateral negativity and ipsilateral positivity with respect to the movement direction at the PPC areas.

### B. EEG Spectral Modulation

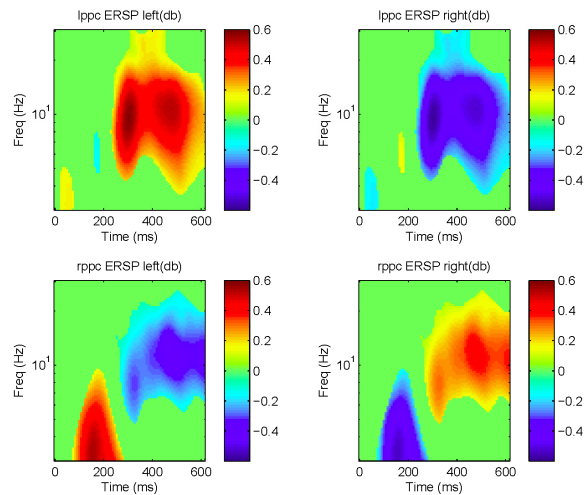


Figure 3. Group-averaged ERSPs for two PPC electrodes (upper row: left PPC electrode, lower row: right PPC electrode) under the reach left (left column) and reach right (right column) conditions. ERSPs were normalized by subtracting the mean baseline log power spectrum of the two conditions from each spectral estimate.

Time-frequency distributions of the EEG spectral power were calculated using event-related spectral perturbation (ERSP) [11]. As shown in Fig. 3, after 300ms, the ERSP images showed a significant contralateral decrease and ipsilateral increase of alpha-band power with respect to the movement direction, which is consistent with the findings in previous visuospatial attention studies [9]. Furthermore, in the right PPC area, the theta-band power also showed a significant difference around 200ms, which behaved differently from the alpha-power modulation. The power modulation of the theta-band activities occurred at the same time window as the ERP modulation; therefore, it might reflect the process of visuomotor transformation.

### C. Classification Accuracy

TABLE I. TEN-FOLD CROSS-VALIDATION ACCURACIES FOR USING THREE DIFFERENT KINDS OF FEATURES.

Subject	Cross-Validation Accuracy		
	ERP Features	Spectral Features	Combined Features
1	65.00	61.43	66.43
2	69.29	70.00	77.86
3	67.14	66.43	65.71
4	65.71	65.71	72.86
5	68.57	57.14	71.43
6	49.29	62.14	62.86
7	63.57	63.57	58.57
8	66.43	66.43	72.14
9	72.14	80.00	75.00
10	67.14	62.86	74.29
Mean	65.43	65.57	69.71

Table I lists the results of cross-validation assessment for the three different types of features. On average, the classification accuracy using ERP and spectral features was comparable (65.4% vs. 65.6%). The combined features achieved an improvement to 69.7%. A paired one-tailed t-test showed that the improvement is statistically significant (combined features vs. ERP features:  $p=0.015$ ; combined features vs. spectral features:  $p=0.038$ ). These results verified the hypothesis that ERP and EEG spectral features provide complementary information for decoding intended movement direction, and thus, significantly improve the classification accuracy through feature combination. The accuracy improvement was found in most of the subjects. In particular, Subjects 2, 4 and 10 had a significant improvement of 7-8% when using combined features. However, some subjects (e.g., Subject 7) showed no performance improvement, which might be attributed to the decrease of generalization ability of the classifier due to the increase of the feature dimension in feature combination. To improve the generalization ability of the classifier (i.e., avoid the curse of dimensionality) and reduce the computational requirements, one way is to further reduce the dimension of spectral power features through temporal averaging. Another potential solution is to apply a meta-level classifier to the continuous outputs of the

individual classifiers on each single feature vector [15]. For example, instead of the simple feature concatenation approach, a linear discriminant analysis classifier can be used to classify the output probabilities from the two base-level SVM classifiers based on ERP features and spectral features, respectively.

## IV. CONCLUSION

This study designed a delayed movement paradigm to investigate brain activities in the human PPC during planning of movements. Experimental results showed that EEG signals generated in the PPC areas carry information about intended movement direction. This study also tested the feasibility of decoding movement intention by combining ERPs and EEG spectral changes in the PPC areas. The resulting classification accuracy (~70%) at the single-trial level suggested the practical potential of an EEG-based BCI for decoding movement intention.

## REFERENCES

- [1] M. A. Lebedev and M. A. L. Nicolelis, "Brain-machine interfaces: past, present and future," *Trends Neurosci.*, vol. 29, no. 9, pp. 536-546, 2006.
- [2] D. M. Taylor, S. I. H. Tillery, and A. B. Schwartz, "Direct cortical control of 3D neuroprosthetic devices," *Science*, vol. 296, no. 5574, pp. 1829-1832, 2002.
- [3] M. A. L. Nicolelis, "Actions from thoughts," *Nature*, vol. 409, no. 18, pp. 403-40, 2001.
- [4] L. R. Hochberg, M. D. Serruya, G. M. Friehs, J. A. Mukand, M. Saleh, A. H. Caplan, A. Branner, D. Chen, R. D. Penn, and J. P. Donoghue, "Neuronal ensemble control of prosthetic devices by a human with tetraplegia," *Nature*, vol. 442, no. 7099, pp. 164-171, 2006.
- [5] R. Q. Quiroga, L. H. Snyder, A. P. Bastista, and R. A. Andersen, "Movement intention is better predicted than attention in the posterior parietal cortex," *J. Neurosci.*, vol. 26, no. 13, pp. 3615-3620, 2006.
- [6] P. S. Hammon, S. Makeig, H. Poizner, E. Todorov, and V. R. de Sa, "Predicting reaching targets from human EEG," *IEEE Signal Process. Mag.*, vol. 25, no. 1, pp. 69-77, 2008.
- [7] S. Waldert, H. Preissl, E. Demandt, C. Braun, N. Birbaumer, A. Aertsen, and C. Mehring, "Hand movement direction decoded from MEG and EEG," *J. Neurosci.*, vol. 28, no. 4, pp. 1000-1008, 2008.
- [8] Y. Wang and S. Makeig, "Predicting intended movement direction using EEG from human posterior parietal cortex," in *2009 D.D. Schmorow et al. (Eds.): Augmented Cognition, HCII 2009, LNAI vol. 5638*, pp. 437-446.
- [9] G. Thut, A. Nietzel, S. A. Brandt, and A. Pascual-Leone, "Alpha-band electroencephalographic activity over occipital cortex indexes visuospatial attention bias and predicts visual target detection," *J. Neurosci.*, vol. 26, no. 37, pp. 9494-9502, 2006.
- [10] T. P. Jung, S. Makeig, C. Humphries, T. W. Lee, M. J. McKeown, V. Iragui, and T. J. Sejnowski, "removing electroencephalographic artifacts by blind source separation," *Psychophysiology*, vol. 37, pp. 163-178, 2000.
- [11] A. Delorme, S. Makeig, "EEGLAB: an open source toolbox for analysis of single-trial EEG dynamics including independent component analysis," *J. Neurosci. Meth.*, vol. 134, pp. 9-21, 2004.
- [12] V. Vapnik, *The Nature of Statistical Learning Theory*. New York: Springer-Verlag, 1995.
- [13] W. K. Härdle and L. Simar, *Applied Multivariate Statistical Analysis*. in 3rd ed., Berlin Heidelberg: Springer-Verlag, 2012, pp. 385-395.
- [14] A. V. Oppenheim and R. W. Schaffer, *Discrete-Time Signal Processing*. Englewood Cliffs, NJ: Prentice-Hall, 1989, pp. 713-718.
- [15] G. Dornhege, B. Blankertz, G. Curio, and K. R. Muller, "Boosting bit rates in noninvasive EEG single-trial classifications by feature combination and multiclass paradigms," *IEEE Trans. Biomed. Eng.*, vol. 51, no. 6, pp. 993-1002, 2004.